16. D. Morishita, R. Katayama, K. Sekimizu, T. Tsuruo, N. Fujita, *Cancer Res.* **68**, 5076–5085 (2008).
17. R. J. Sheaff, M. Groudine, M. Gordon, J. M. Roberts, B. E. Clurman, *Genes Dev.* **11**, 1464–1478 (1997).
18. J. D. Keene, *Nat. Rev. Genet.* **8**, 533–543 (2007).
19. N. Herranz *et al.*, *Nat. Cell Biol.* **17**, 1205–1217 (2015).
20. K. Ochiai *et al.*, *Nat. Immunol.* **13**, 300–307 (2012).
21. A. B. Cooper *et al.*, *Nat. Immunol.* **7**, 489–497 (2006).
22. B. J. Thompson *et al.*, *J. Exp. Med.* **212**, 953–970 (2015).
23. M. Marderosian *et al.*, *Oncogene* **25**, 6277–6290 (2006).
24. D. J. Stumpo *et al.*, *Blood* **114**, 2401–2410 (2009).
25. M. A. Hausburg *et al.*, *eLife* **4**, e03390 (2015).
26. A. S. Halees, R. El-Badrawi, K. S. Khabar, *Nucleic Acids Res.* **36**, D137–D140 (2008).
27. G. Yao, T. J. Lee, S. Mori, J. R. Nevins, L. You, *Nat. Cell Biol.* **10**, 476–482 (2008).
28. D. Resnitzky, S. I. Reed, *Mol. Cell. Biol.* **15**, 3463–3469 (1995).
29. E. Vigo *et al.*, *Mol. Cell. Biol.* **19**, 6379–6395 (1999).
30. G. Leone, J. DeGregori, L. Jakoi, J. G. Cook, J. R. Nevins, *Proc. Natl. Acad. Sci. U.S.A.* **96**, 6626–6631 (1999).
31. A. C. Minella *et al.*, *Genes Dev.* **22**, 1677–1689 (2008).

ACKNOWLEDGMENTS

We thank K. Vogel, R. Newman, C. Tiedje, and S. Bell for advice and comments on the manuscript; L. Matheson, A. Stark, and R. Venigalla for technical advice; S. Bell, K. Bates, D. Sanger, N. Evans, and The Babraham Institute's Biological Support Unit, Flow Cytometry Core Facility, and Next Generation Sequencing Facility for expert technical assistance; J. Ule and T. Curk for help with iCLIP; L. Dolken for the gateway-compatible psi-check vector; and R. Brink, D. Kioussis, and M. Reth for mice. This work was funded by the Biotechnology and Biological Sciences Research Council, a Medical Research Council (MRC) Collaborative Award in Science and Engineering (CASE) studentship with GlaxoSmithKline, a MRC centenary award (A.G.), and project grants from Bloodwise. D.J.H. was supported by a MRC Clinician Scientist Fellowship. The data from this study are tabulated in the main paper and in the supplementary materials. Sequencing data from the RNA sequencing and iCLIP experiments have been deposited in the National Center for Biotechnology Information's Gene Expression Omnibus (GEO) and are accessible under GEO Series accession number GSE78249 (www.ncbi.nlm.nih.gov/geo/query/acc.cgi?acc=GSE78249). *Zfp36l1*^{fl}, *Zfp36l2*^{fl}, and *ROSA26*^{L1} mice are available from The Babraham Institute under a material transfer agreement.

SUPPLEMENTARY MATERIALS

www.sciencemag.org/content/352/6284/453/suppl/DC1
Materials and Methods
Figs. S1 to S13
Tables S1 to S16
References (*32*–*50*)

7 October 2015; accepted 26 February 2016
10.1126/science.aad5978

IMMUNOLOGY

Hobit and Blimp1 instruct a universal transcriptional program of tissue residency in lymphocytes

Laura K. Mackay,[1,2]† Martina Minnich,[3] Natasja A. M. Kragten,[4] Yang Liao,[5,6] Benjamin Nota,[7] Cyril Seillet,[5,6] Ali Zaid,[1] Kevin Man,[5,6] Simon Preston,[5,6] David Freestone,[1] Asolina Braun,[1] Erica Wynne-Jones,[1] Felix M. Behr,[4,5,6,8] Regina Stark,[4] Daniel G. Pellicci,[1,2] Dale I. Godfrey,[1,2] Gabrielle T. Belz,[5,6] Marc Pellegrini,[5,6] Thomas Gebhardt,[1] Meinrad Busslinger,[3] Wei Shi,[5,9] Francis R. Carbone,[1] René A. W. van Lier,[4] Axel Kallies,[5,6]*† Klaas P. J. M. van Gisbergen[4,5,6,8]*†

Tissue-resident memory T (Trm) cells permanently localize to portals of pathogen entry, where they provide immediate protection against reinfection. To enforce tissue retention, Trm cells up-regulate CD69 and down-regulate molecules associated with tissue egress; however, a Trm-specific transcriptional regulator has not been identified. Here, we show that the transcription factor Hobit is specifically up-regulated in Trm cells and, together with related Blimp1, mediates the development of Trm cells in skin, gut, liver, and kidney in mice. The Hobit-Blimp1 transcriptional module is also required for other populations of tissue-resident lymphocytes, including natural killer T (NKT) cells and liver-resident NK cells, all of which share a common transcriptional program. Our results identify Hobit and Blimp1 as central regulators of this universal program that instructs tissue retention in diverse tissue-resident lymphocyte populations.

We recently identified a core set of genes specifically associated with tissue residency of CD8 T cells (*1*). Genes up-regulated in Trm cells included *Zfp683* (*LOC100503878*), also termed "homolog of Blimp1 in T cells" (Hobit), a transcription factor that we previously identified in NKT cells (*2*). Virus-specific CD8 T cells in skin, but not spleen, after herpes simplex virus (HSV) infection expressed large amounts of *Hobit* transcripts (Fig. 1A). *Hobit* expression in skin T cells was low at day 8 and high by day 30 postinfection (p.i.) (Fig. 1A). This was in contrast to *Prdm1* (hereafter, *Blimp1*), which peaked at day 8 p.i. and persisted at lower levels in splenic and skin memory CD8 T cells (Fig. 1B). Similarly, after acute infection with lymphocytic choriomeningitis virus (LCMV), *Hobit* was specifically induced in gut Trm cells, whereas *Blimp1* was expressed ubiquitously in memory CD8 T cells (fig. S1, A and B). Thus, within the CD8 T cell lineage, Hobit is expressed in a Trm-specific manner.

To examine the function of Hobit and Blimp1 in Trm cell differentiation, we used a mouse model to generate skin Trm cells, by the intradermal injection of activated CD8 T cells, as previously described (*1*). After transfer, wild-type (WT) CD8 T cells persisted in skin and acquired a Trm phenotype (Fig. 1, C and D, and fig. S2A). Cotransferred Hobit-deficient CD8 T cells were reduced in skin, despite similar maintenance in spleen, as compared with WT cells (Fig. 1C), which suggested that Hobit was specifically required for Trm cell development. Blimp1 was not essential for skin Trm cell formation by itself, but collaborated with Hobit in a synergistic manner (Fig. 1C and fig. S2, A and B). Residual *Hobit* and *Blimp1* doubly deficient [double-knockout (DKO)] CD8 T cells in the skin displayed reduced surface expression of Trm cell–associated molecules compared with WT CD8 T cells (Fig. 1D and fig. S2C). To study Trm cell development during viral infection, we infected mice with HSV and analyzed endogenous CD8 T cell responses. We used mixed–bone marrow (BM) chimeric mice, containing WT and mutant compartments at a 1:1 ratio, to minimize indirect effects through differences in viral clearance. This ratio was largely maintained in the antigen-specific CD8 T cells, regardless of location at the peak of the T cell response (Fig. 1E). In line with previous findings (*3*, *4*), Blimp1, but not Hobit, was required for the formation of short-lived effectors and granzyme B expression, which resulted in increased proportions of Blimp1-deficient memory precursors (fig. S3, A and B, and fig. S4, A to G) and memory CD8 T cells (Fig. 1, E and F). The combined loss of Hobit and Blimp1 strongly compromised development of skin Trm cells but not of circulating memory cells (Fig. 1, E and F). After infection with LCMV, double deficiency in Hobit and Blimp1 abrogated the development of gut-resident CD8 T cells but not of splenic CD8 T cells (fig. S5, A and B). Thus, Hobit and Blimp1 cooperate to specifically promote Trm development.

Tissue residency has also been described for innate lymphocytes, including subpopulations of NK and NKT cells (*5*–*8*). Tissue-resident NK

[1]Department of Microbiology and Immunology, The University of Melbourne, The Peter Doherty Institute for Infection and Immunity, Melbourne, Australia. [2]Australian Research Council (ARC) Centre of Excellence in Advanced Molecular Imaging, University of Melbourne, Melbourne, Australia. [3]Research Institute of Molecular Pathology (IMP), Vienna Biocenter (VBC), Vienna, Austria. [4]Department of Hematopoiesis, Sanquin Research and Landsteiner Laboratory, Academic Medical Center (AMC), University of Amsterdam, Amsterdam, Netherlands. [5]The Walter and Eliza Hall Institute of Medical Research, Melbourne, Australia. [6]Department of Medical Biology, The University of Melbourne, Melbourne, Australia. [7]Department of Blood Cell Research, Sanquin Research and Landsteiner Laboratory, AMC, University of Amsterdam, Amsterdam, Netherlands. [8]Department of Experimental Immunology, AMC, Amsterdam, Netherlands. [9]Department of Computing and Information Systems, The University of Melbourne, Melbourne, Australia.
*These authors contributed equally to this work. **†Corresponding author. Email: lkmackay@unimelb.edu.au (L.K.M.); kallies@wehi.edu.au (A.K.); k.vangisbergen@sanquin.nl (K.P.J.M.v.G.)**

(trNK) cells in the liver, also known as type 1 innate lymphoid cells (ILC1), can be distinguished from conventional NK (cNK) cells through expression of the Trm cell–associated molecules CD49a and CD69 (*7*, *9*–*11*). Liver trNK cells expressed *Hobit* to a similar extent as NKT cells, whereas cNK cells did not (Fig. 2A). In contrast, *Blimp1* was highly expressed in circulating cNK cells compared with trNK and NKT cells (Fig. 2B and fig. S6A). In line with this expression pattern, trNK cells in liver, but not cNK cells in liver or spleen, were Hobit dependent (Fig. 2, C to E, and fig. S6B). In contrast, cNK cells in liver were dependent on Blimp1, as previously shown (*12*). NKT cells are maintained as resident cells in thymus, spleen, and liver (*5*, *8*). As were Trm cells, NKT cells were largely positive for CD49a and CD69 (fig. S7, A and B) and expressed *Hobit* and *Blimp1* (Fig. 2A and fig. S7C). Numbers of splenic and liver NKT cells were not substantially different in mice lacking either Hobit or Blimp1. In contrast, NKT cells lacking both Hobit and Blimp1 were reduced in liver, but not spleen, a phenotype that was exacerbated in a competitive setting (Fig. 2, F and G, and fig. S8, A and B). Hobit and Blimp1 were not required for migration but for maintenance of liver NKT cells (fig. S9, A to E). Furthermore, the combined deficiency in Hobit and Blimp1 reduced the proportions of Trm-type NKT cells in spleen (fig. S7, A and B). Thus, Hobit and Blimp1 jointly regulate the development and maintenance of innate tissue-resident lymphocytes.

In line with a recent report (*13*), LCMV induced the differentiation of Trm-phenotype CD8 T cells in the liver that lacked CD103 expression (Fig. 3, A and B, and fig. S10, A to D). $CD103^-$ Trm cells have also been described in other nonbarrier tissues (*13*–*16*), but it is unclear how the differentiation of these cells relates to that of $CD103^+$ Trm cells at epithelial sites. As were $CD103^+$ Trm cells, liver-derived Trm cells expressed and required both Hobit and Blimp1 for differentiation (Fig. 3, C and D, and fig. S10, E and F), as did the $CD103^-$ Trm population in kidney (fig. S10, G and H). Thus, resident lymphocytes at nonepithelial sites also require Hobit and Blimp1 for development. Previously, we have shown that interleukin-15 (IL-15) and the transcription factor T-bet mediate Trm cell development and/or maintenance (*17*). Trm cells had reduced *Hobit* expression in an IL-15–deficient environment, and activated CD8 T cells up-regulated Hobit in response to IL-15 in a T-bet–dependent manner (fig. S11, A and B). Overexpression of T-bet induced *Hobit* expression (fig. S11, B and C), which suggested that T-bet was both essential and sufficient. In contrast, *Blimp1* expression is not induced by IL-15 or T-bet (*18*). Transforming growth factor-β, which is also associated with Trm cell differentiation, did not induce *Hobit* expression (fig. S11B). In support of these notions, NKT1 cells, which depend on T-bet and IL-15 (*19*), but not NKT2 cells, expressed *Hobit* and *Blimp1* and displayed a phenotype consistent with tissue residency (fig. S12, A to C). These findings suggest that the molecular circuits that drive tissue residency are conserved between lymphocyte populations.

To identify a lineage-independent gene signature of tissue residency, we performed genome-wide transcriptional profiling. Antigen-specific Trm cells from the skin and gut of mice that were infected with HSV or LCMV, respectively, were compared with circulating $CD8^+$ central memory T cells (Tcm) and effector memory T cells (Tem) of the same specificity. We obtained a set of 192 genes whose specific up- or down-regulation was associated with $CD103^+$ Trm cells (fig. S13A). The gene expression profile of $CD103^-$ LCMV-specific

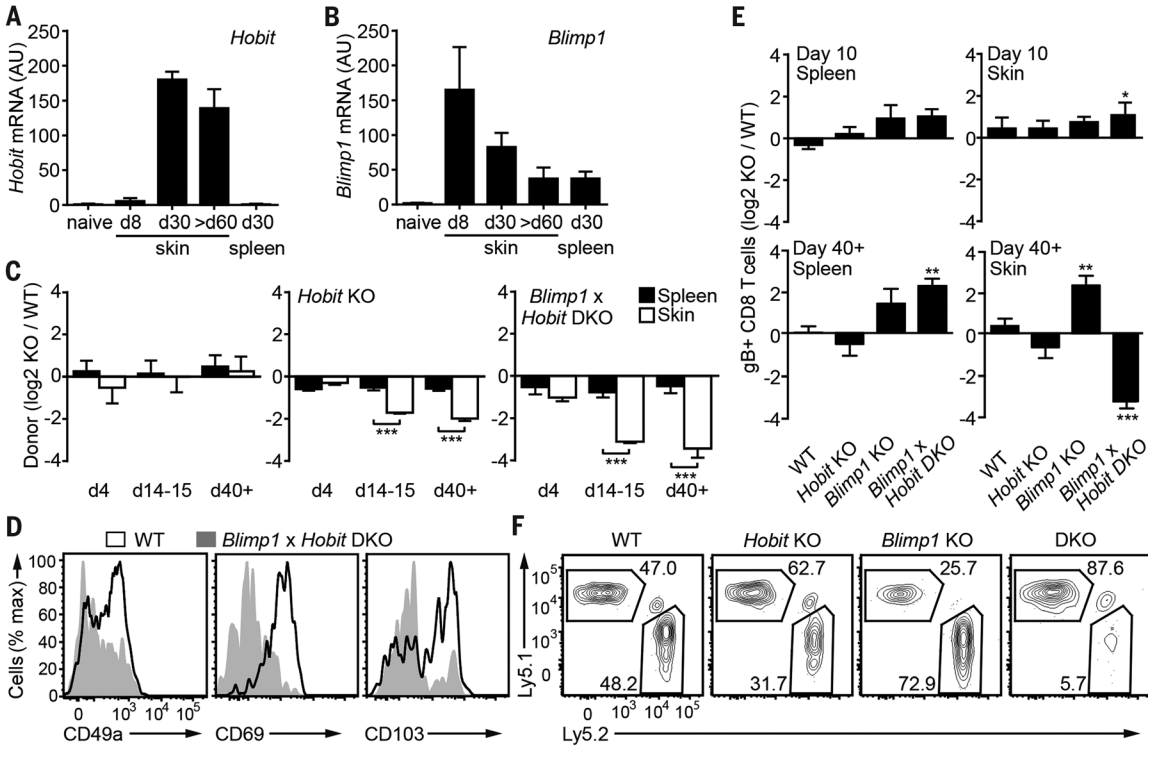

Fig. 1. Hobit and Blimp1 regulate the maintenance of Trm cells within the skin. (**A**) *Hobit* and (**B**) *Blimp1* expression in naïve and HSV glycoprotein B (gB)–specific CD8 T cell receptor transgenic T cells from skin and spleen at effector (day 8 p.i.) and memory (after day 30 p.i.) time points after HSV infection. AU, arbitrary units. (**C** and **D**) Activated congenically marked CD8 T cells from WT mice were cotransferred at a 1:1 ratio with *Blimp1*-deficient [knockout (KO)] (right), *Hobit* KO (center), or *Blimp1* × *Hobit* DKO CD8 T cells (left) into Ly5.1-recipient mice by intradermal injection. (C) Ratio (log2) of transferred WT and mutant CD8 T cells in spleen and skin at the indicated time points after transfer (d, day). (D) CD49a (left), CD69 (center), and CD103 (right) expression in donor WT (black line) and *Blimp1* × *Hobit* DKO CD8 T cells (filled gray) 14 to 15 days posttransfer. (**E** and **F**) Mixed-BM chimeric mice containing congenically marked WT ($Ly5.1^+$) and control WT, *Hobit* KO, *Blimp1* KO, or *Blimp1* × *Hobit* DKO cells ($Ly5.2^+$) were infected with HSV, and antigen-specific CD8 T cells were enumerated in spleen and skin using gB tetramer. (E) The ratio (log2) of gB^+ WT and mutant CD8 T cells at effector (day 10 p.i.) and memory (day 40+ p.i.) times in spleen and skin. Ratio of $CD103^+$ gB^+ CD8 T cells is shown in skin at day 40+ p.i. (bottom right). (F) WT and the indicated WT or mutant HSV-specific CD8 T cells were detected in the skin of mixed-BM chimeric mice at day 40+ p.i. by Ly5.1 and Ly5.2 expression, respectively. Plots were gated on $CD103^+$ gB^+ Trm cells. Data in (A) and (B) represent pooled results from three to six mice per group; data in (C) and (D) are pooled from two independent experiments with six to eight mice per time point; data in (E) and (F) are representative of two independent experiments with four or five mice per group. $^*P < 0.05$, $^{**}P < 0.01$, $^{***}P < 0.001$, as determined by two-tailed Student's *t* test (C) or by one-sample Student's *t* test (E). Error bars denote means ± SEM.

liver Trm cells showed that they did not equilibrate with circulating Tem in spleen or liver (fig. S13B). Genes associated with CD103$^+$ Trm were significantly enriched in liver Trm cells (fig. S13, C and D), which demonstrated overlap in the transcriptional profile of Trm cells at epithelial and nonepithelial sites. A significant fraction of the gene signature of epithelial Trm was also retained in trNK and NKT cells compared with

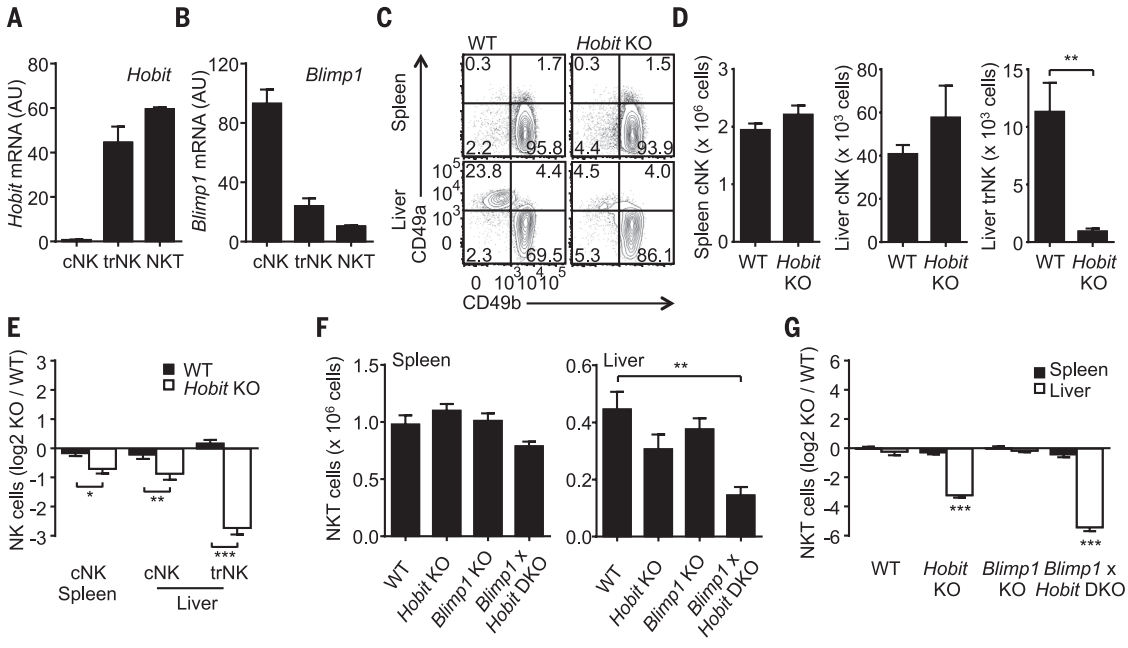

Fig. 2. Hobit and Blimp1 regulate the maintenance of liver-resident NK and NKT cells. (**A**) Hobit and (**B**) Blimp1 expression in cNK, trNK, and NKT cells from the liver. (**C**) Expression of CD49a and CD49b on spleen and liver NK cells (gated as TCRβ$^-$NK1.1$^+$) of WT (left) and *Hobit* KO mice (right). (**D**) Numbers of splenic cNK (left), liver cNK (center), and liver trNK (right) in WT and *Hobit* KO mice. (**E**) Ratio (log2) of WT and *Hobit* KO cNK and trNK cells in spleen and liver in mixed-BM chimeric mice. (**F**) Numbers of splenic (left) or liver NKT cells (right) from WT, *Hobit* KO, *Blimp1* KO, and *Blimp1* × *Hobit* DKO mice. (**G**) Ratio (log2) of the indicated WT and mutant NKT cells from spleen and liver in mixed-BM chimeric mice. (A) and (B), pooled results with three mice per group; (C) to (E), pooled results from two independent experiments of 6 to 7 mice per group; (F), pooled from three independent experiments with 6 to 11 mice per group; and (G), pooled from four independent experiments with 6 mice per group. *P < 0.05, **P < 0.01, ***P < 0.001, as determined by two-tailed Student's t test (D) and (E), by one-way ANOVA (F), or by one-sample Student's t test (G). Error bars denote means ± SEM.

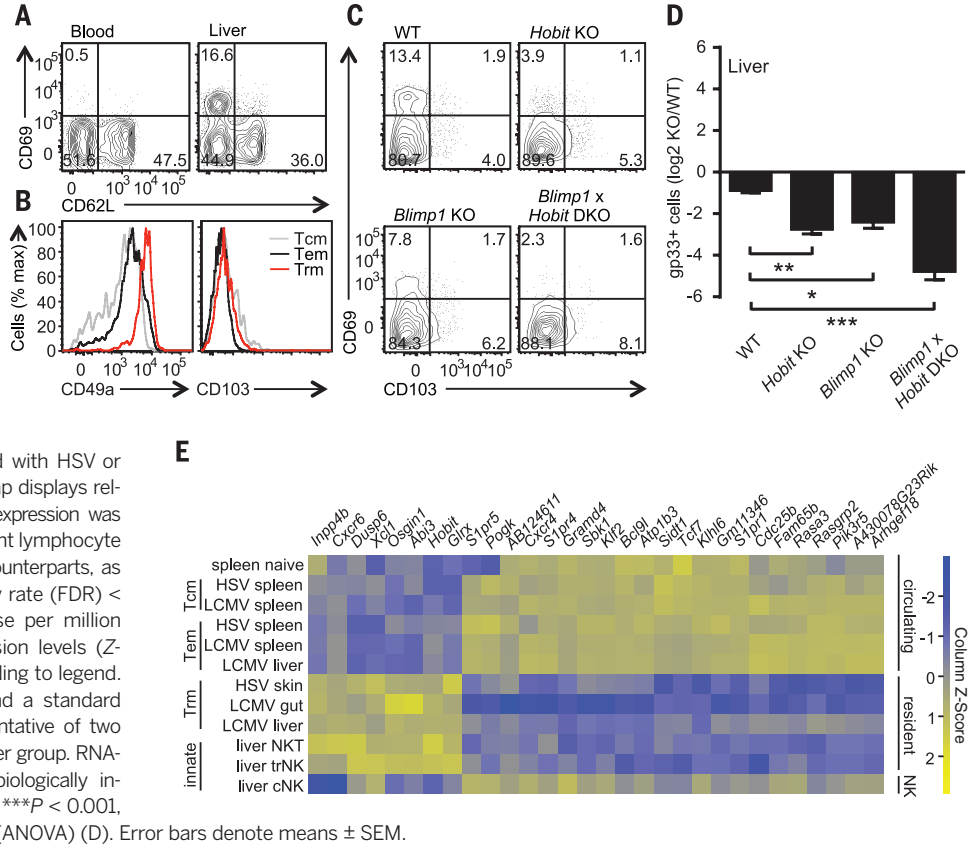

Fig. 3. Identification of a universal transcriptional program of lymphocyte tissue residency including CD103$^+$ Trm, CD103$^-$ liver Trm, and innate lymphocytes. (**A**) Expression of CD62L and CD69 on LCMV-specific [glycoprotein 33–positive (gp33$^+$)] CD8 T cells in blood and liver at day 40+ p.i. after LCMV. (**B**) CD49a and CD103 expression on CD62L$^+$CD69$^-$ Tcm (gray line), CD62L$^-$CD69$^-$ Tem (black line), and CD62L$^-$CD69$^+$ Trm cells (red line) from the liver. (**C**) Phenotype of LCMV-specific CD8 T cells and (**D**) ratio (log2) of CD69$^+$ LCMV-specific CD8 T cells of the indicated genotypes from the liver of mixed-BM chimeric mice at day 50+ after infection with LCMV. (**E**) Naïve CD8 T cells, cNK, trNK, and NKT cells were sorted from naïve mice, and Tcm, Tem, and Trm populations were sorted from indicated tissues of mice infected with HSV or LCMV at day 40+ p.i. (memory phase). Heat map displays relative amounts of transcripts of genes, whose expression was specifically up- or down-regulated in tissue-resident lymphocyte populations in comparison to their circulating counterparts, as determined by RNA sequencing [false discovery rate (FDR) < 0.05; fold change > 2; and reads per kilobase per million mapped reads (RPKM) > 8]. Relative expression levels (Z-scores) of genes are shown, color-coded according to legend. Columns are scaled to have a mean of 0 and a standard deviation of 1. Data in (A) to (D) are representative of two independent experiments with four to six mice per group. RNA-sequencing data in (E) is pooled from two biologically independent experiments. *P < 0.05, **P < 0.01, ***P < 0.001, as determined by one-way analysis of variance (ANOVA) (D). Error bars denote means ± SEM.

their circulating counterparts (fig. S14, A to C), which suggested that innate and adaptive lymphocytes establish tissue residency in a similar manner. We identified 30 genes, whose expression pattern was specifically associated with tissue residency independent of lineage or tissue of origin (Fig. 3E). This signature included genes required for tissue egress, such as *Klf2* and *S1pr1*, which were tightly down-regulated in resident populations (Fig. 3E). Similarly, down-regulation of *Tcf7*, encoding transcription factor TCF1 and associated with development of circulating memory (*20*–*22*), was a common feature of resident lymphocyte populations (Fig. 3E). Note that *Hobit* was the only transcription factor specifically up-regulated in this gene set (Fig. 3E), which underlined its unique position in the transcriptional regulation of tissue-resident lymphocytes.

Hobit and Blimp1 are highly homologous in their DNA-binding zinc finger domains (*2*, *23*), which suggested overlapping roles in transcriptional regulation. To determine how Hobit and Blimp1 control tissue residency, we used cultured NKT cells that expressed large amounts of *Hobit* and *Blimp1* compared with similarly cultured CD8 T cells (fig. S15A). Consistent with the phenotype of tissue-resident cells, WT NKT cells expressed CD69, whereas NKT cells lacking Hobit and Blimp1 did not (fig. S15B). The combined loss of Hobit and Blimp1 caused the deregulated expression of a large number of genes (Fig. 4A), which suggested that Hobit and Blimp1 coregulate gene expression in a highly synergistic manner. Signature genes of tissue residency were enriched within Hobit- and Blimp1-regulated genes and included *Klf2*, *S1pr1*, and *Tcf7*, which were derepressed in the combined absence of Hobit and Blimp1 (Fig. 4B; fig. S15C; and fig. S16, A and B). We also observed derepression of *Ccr7* (Fig. 4B and fig. S16C), which is required for lymphocyte egress from peripheral tissues (*24*, *25*). WT NKT cells did not migrate toward S1P, the ligand for sphingosine-1-phosphate receptor 1 (S1PR1), or CCL21, the ligand for CCR7. In contrast, NKT cells lacking both Blimp1 and Hobit were highly responsive to both chemotactic stimuli (Fig. 4, C and D). In line with this migratory behavior, *Hobit* and *Blimp1* DKO NKT cells localized preferentially to the white pulp and were largely absent from the red pulp of spleen (fig. S16, D to G). To identify directly regulated genes, we performed chromatin immunoprecipitation (ChIP) sequencing using CD8 T cells expressing biotin-tagged Blimp1 (*26*) or V5-tagged

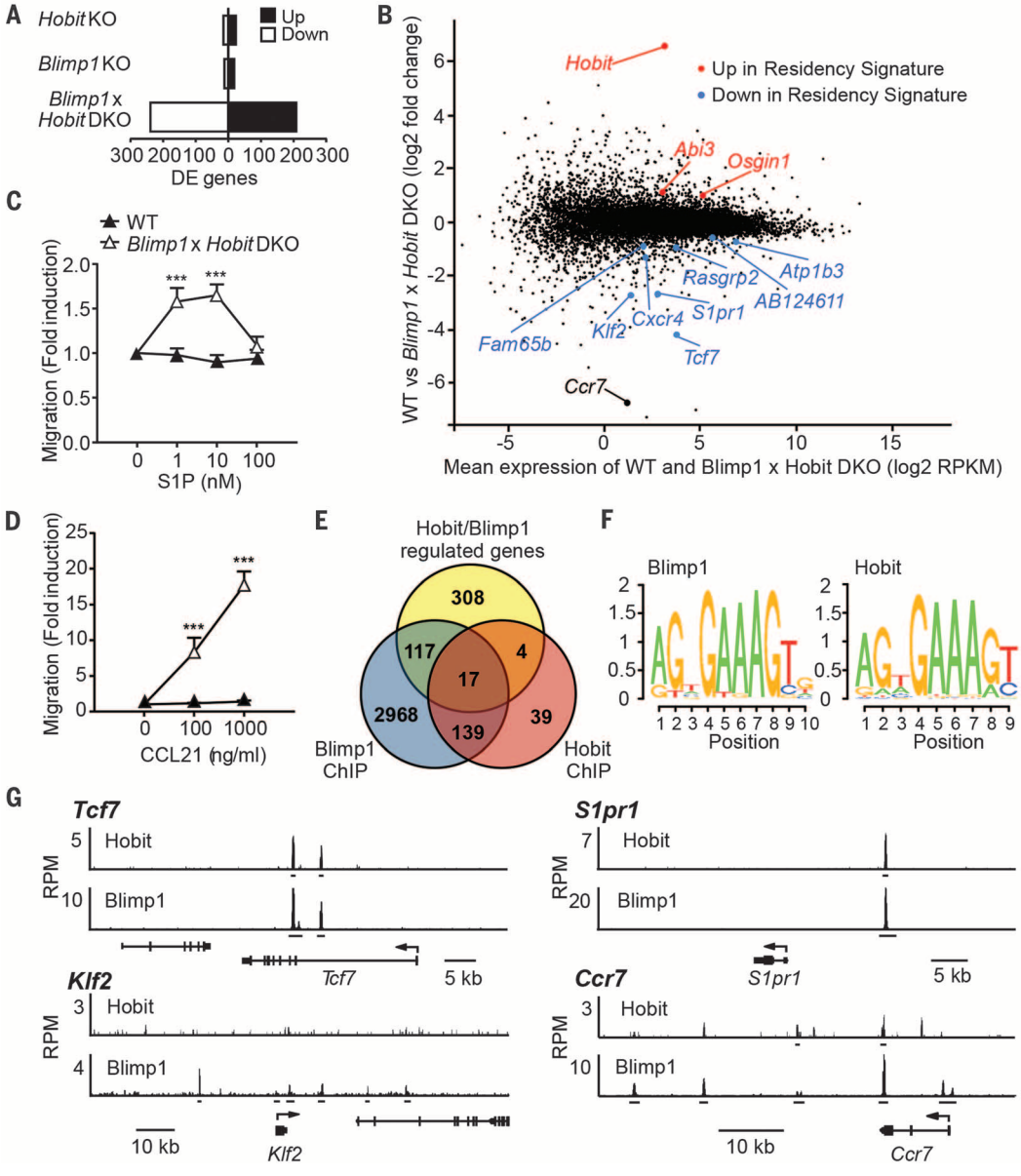

Fig. 4. Hobit and Blimp1 cooperate to repress genes required for tissue egress. (**A** and **B**) WT, *Hobit* KO, *Blimp1* KO, and *Blimp1* × *Hobit* DKO NKT cells were analyzed by RNA sequencing. DE, differentially expressed. (A) The number of significantly up- (black bars) or down-regulated genes (white bars) in mutant compared with WT NKT cells, as indicated (FDR < 0.05; fold change > 1.5; RPKM > 4). (B) Scatter plot displays log2 fold changes of WT versus *Blimp1* × *Hobit* DKO (*y* axis) against the mean expression level (*x* axis) for all expressed genes. Up-regulated tissue residency signature genes are marked in red, down-regulated tissue residency genes in blue, and *Ccr7* in black. (**C** and **D**) Migration of WT and *Blimp1* × *Hobit* DKO NKT cells in response to (C) S1PR1 ligand S1P and (D) CCR7 ligand CCL21. (**E**) Venn diagram displays the overlap between genes bound by either Hobit or Blimp1 in CD8 T cells, as identified by ChIP sequencing, and genes differentially expressed between WT and *Blimp1* × *Hobit* DKO NKT cells. (**F**) The DNA-binding motif of Blimp1 (left) and Hobit (right) was determined by sequence analysis of binding regions. (**G**) ChIP-sequencing tracks show binding of Hobit or Blimp1 to *Tcf7*, *Klf2*, *S1pr1*, and *Ccr7* as indicated in CD8 T cells. Significant binding regions are marked by horizontal lines. RPM, reads per million. Data in (A) and (B) are pooled from three independent experiments; data in (C) and (D) display pooled results of three or four independent experiments; data in (E) to (G) are based on one Hobit and Blimp1 ChIP-sequencing experiment each. ***$P < 0.001$ as determined by two-tailed Student's *t* test (C) and (D).

Hobit. We identified 4510 genome-wide binding sites for Blimp1, which could be assigned to 3241 genes. Hobit bound 404 sites, >50% of which overlapped with Blimp1 (fig. S17). Note that 78% of the 199 genes bound by Hobit were also bound by Blimp1, whereas 31% of the genes deregulated in the absence of Hobit and Blimp1 were bound by Hobit, Blimp1, or both (Fig. 4E). Hobit and Blimp1 used nearly identical binding motifs (Fig. 4F), which supports the notion of extensive cooperation between both factors. Hobit and Blimp1 bound target sequences within the *S1pr1*, *Ccr7*, and *Tcf7* loci, which suggested direct repression of these genes (Fig. 4G). In addition, Blimp1, but not Hobit, bound within the *Klf2* locus (Fig. 4G). Thus, Hobit and Blimp1 mediate a transcriptional program of tissue residency that is shared among Trm, trNK, and NKT cells and includes the suppression of tissue egress genes.

The recent recognition of Trm cells as essential sentinels at barrier tissues (*27*–*30*) highlights the importance of understanding their development. We have characterized a universal transcriptional program of tissue residency that is shared between adaptive and innate lymphocytes at both epithelial and nonepithelial sites. Our findings reveal the central roles of Hobit and Blimp1 in the establishment of tissue residency and indicate that they function by silencing lymphocyte egress from the tissues and by repressing the development of circulating memory cells. The key insights into the transcriptional regulation of Trm cells within this study may assist in the manipulation of tissue-resident memory for the development of vaccine strategies to improve localized immunity.

REFERENCES AND NOTES

1. L. K. Mackay *et al.*, *Nat. Immunol.* **14**, 1294–1301 (2013).
2. K. P. van Gisbergen *et al.*, *Nat. Immunol.* **13**, 864–871 (2012).
3. A. Kallies, A. Xin, G. T. Belz, S. L. Nutt, *Immunity* **31**, 283–295 (2009).
4. R. L. Rutishauser *et al.*, *Immunity* **31**, 296–308 (2009).
5. S. P. Berzins, F. W. McNab, C. M. Jones, M. J. Smyth, D. I. Godfrey, *J. Immunol.* **176**, 4059–4065 (2006).
6. G. Gasteiger, X. Fan, S. Dikiy, S. Y. Lee, A. Y. Rudensky, *Science* **350**, 981–985 (2015).
7. D. K. Sojka *et al.*, *eLife* **3**, e01659 (2014).
8. S. Y. Thomas *et al.*, *J. Exp. Med.* **208**, 1179–1188 (2011).
9. C. Daussy *et al.*, *J. Exp. Med.* **211**, 563–577 (2014).
10. S. M. Gordon *et al.*, *Immunity* **36**, 55–67 (2012).
11. M. L. Robinette *et al.*, *Nat. Immunol.* **16**, 306–317 (2015).
12. A. Kallies *et al.*, *Blood* **117**, 1869–1879 (2011).
13. E. M. Steinert *et al.*, *Cell* **161**, 737–749 (2015).
14. J. M. Schenkel, K. A. Fraser, D. Masopust, *J. Immunol.* **192**, 2961–2964 (2014).
15. L. M. Wakim, A. Woodward-Davis, M. J. Bevan, *Proc. Natl. Acad. Sci. U.S.A.* **107**, 17872–17879 (2010).
16. L. M. Wakim *et al.*, *J. Immunol.* **189**, 3462–3471 (2012).
17. L. K. Mackay *et al.*, *Immunity* **43**, 1101–1111 (2015).
18. A. Xin *et al.*, *Nat. Immunol.* **17**, 422–432 (2016).
19. Y. J. Lee, K. L. Holzapfel, J. Zhu, S. C. Jameson, K. A. Hogquist, *Nat. Immunol.* **14**, 1146–1154 (2013).
20. L. Gattinoni *et al.*, *Nat. Med.* **15**, 808–813 (2009).
21. G. Jeannet *et al.*, *Proc. Natl. Acad. Sci. U.S.A.* **107**, 9777–9782 (2010).
22. X. Zhou *et al.*, *Immunity* **33**, 229–240 (2010).
23. F. A. Vieira Braga *et al.*, *Eur. J. Immunol.* **45**, 2945–2958 (2015).
24. S. K. Bromley, S. Y. Thomas, A. D. Luster, *Nat. Immunol.* **6**, 895–901 (2005).
25. G. F. Debes *et al.*, *Nat. Immunol.* **6**, 889–894 (2005).
26. M. Minnich *et al.*, *Nat. Immunol.* **17**, 331–343 (2016).
27. S. Ariotti *et al.*, *Science* **346**, 101–105 (2014).
28. T. Gebhardt *et al.*, *Nat. Immunol.* **10**, 524–530 (2009).
29. X. Jiang *et al.*, *Nature* **483**, 227–231 (2012).
30. J. M. Schenkel *et al.*, *Science* **346**, 98–101 (2014).

ACKNOWLEDGMENTS

We wish to thank L. Mackiewicz and R. Gloury for technical support and M. Jaritz for bioinformatics support. The data presented in this manuscript are tabulated in the main paper and in the supplementary materials. RNA and ChIP sequencing data have been made available under accession numbers GSE70813 and GSE79339 at GEO. *Blimp1*-Bio mice are available from M.B. under a material transfer agreement (MTA) with IMP, *Blimp1* KO, *Blimp1*-GFP and *Blimp1* × *Hobit* DKO mice are available from A.K. under an MTA with The Walter and Eliza Hall Institute and *Hobit* KO and *Blimp1* × *Hobit* DKO mice are available from K.P.J.M.v.G. under an MTA with Sanquin Research. L.K.M. was supported by grant DE140100432 from the ARC and grant 1083685 from the National Health and Medical Research Council of Australia (NHMRC). M.M. and M.B. were supported by the Boehringer Ingelheim and a European Research Council Advanced Grant (291740-LymphoControl) from the European Community's Seventh Framework Programme. A.B. was funded by a Fellowship from the German Research Foundation. R.S. was supported by a Fellowship from the Alexander von Humboldt Foundation. W.S. was supported by grant 1023454 from the NHMRC. N.A.M.K. and R.A.W.v.L. were supported by grant 1136 of the Landsteiner Foundation of Blood Transfusion Research. D.G.P. was supported by an NHMRC Early Career Fellowship (1054431), and D.I.G. was supported by an NHMRC Senior Principal Research Fellowship (1020770). G.T.B. was supported by a fellowship from the ARC and grant 1042582 from the NHMRC. A.K. was supported by a fellowship from the Sylvia and Charles Viertel Foundation and a project grant (637345) from the NHMRC. F.M.B. and K.P.J.M.v.G. were supported by Vidi grant 917.13.338 from The Netherlands Organization of Scientific Research. This work was supported by the Victorian State Government Operational Infrastructure Support and Australian Government NHMRC Independent Research Institute Infrastructure Support scheme.

SUPPLEMENTARY MATERIALS

www.sciencemag.org/content/352/6284/459/suppl/DC1
Materials and Methods
Figs. S1 to S17
References (*31*–*44*)

10 August 2015; accepted 21 March 2016
10.1126/science.aad2035

INNATE IMMUNITY

Mx1 reveals innate pathways to antiviral resistance and lethal influenza disease

Padmini S. Pillai,[1] Ryan D. Molony,[1] Kimberly Martinod,[2] Huiping Dong,[1] Iris K. Pang,[1] Michal C. Tal,[1]* Angel G. Solis,[1] Piotr Bielecki,[1] Subhasis Mohanty,[3] Mark Trentalange,[4] Robert J. Homer,[5] Richard A. Flavell,[1,8] Denisa D. Wagner,[2] Ruth R. Montgomery,[6] Albert C. Shaw,[3] Peter Staeheli,[7] Akiko Iwasaki[1,8]†

Influenza A virus (IAV) causes up to half a million deaths worldwide annually, 90% of which occur in older adults. We show that IAV-infected monocytes from older humans have impaired antiviral interferon production but retain intact inflammasome responses. To understand the in vivo consequence, we used mice expressing a functional *Mx* gene encoding a major interferon-induced effector against IAV in humans. In *Mx1*-intact mice with weakened resistance due to deficiencies in *Mavs* and *Tlr7*, we found an elevated respiratory bacterial burden. Notably, mortality in the absence of *Mavs* and *Tlr7* was independent of viral load or MyD88-dependent signaling but dependent on bacterial burden, caspase-1/11, and neutrophil-dependent tissue damage. Therefore, in the context of weakened antiviral resistance, vulnerability to IAV disease is a function of caspase-dependent pathology.

Respiratory infections with influenza A virus (IAV) cause severe morbidity and mortality in humans and animals worldwide. Older humans are highly susceptible to influenza disease. This susceptibility could be due to an inability to mount an effective antiviral response or an incapacity to develop disease tolerance to IAV infection (*1*–*4*). We began by comparing the innate immune pathways engaged by IAV infections in peripheral blood monocytes from young-adult (20- to 30-year-old) and older (65- to 89-year-old) human donors (table S1 and fig. S1A). IAV-infected monocytes from older humans showed intact nuclear factor κB (NF-κB)–dependent proinflammatory cytokine expression and secretion [interleukin (IL)–6] (fig. S1B and Fig. 1A) and robust inflammasome-dependent cytokine expression and secretion (IL-1β) (fig. S1C and Fig. 1B). Type I interferon (IFN) responses to IAV infection, however, were significantly attenuated in older human monocytes (IFN-β) (Fig. 1C). Reduced

[1]Department of Immunobiology, Yale School of Medicine, New Haven, CT 06520, USA. [2]Program in Cellular and Molecular Medicine, Boston Children's Hospital, Harvard Medical School, Boston, MA, USA. [3]Section of Infectious Diseases, Department of Internal Medicine, Yale School of Medicine, New Haven, Connecticut, USA. [4]Department of Internal Medicine, Yale School of Medicine, New Haven, Connecticut, USA. [5]Department of Pathology, Yale School of Medicine, New Haven, CT 06520, USA. [6]Section of Rheumatology, Department of Internal Medicine, Yale School of Medicine, New Haven, CT 06520, USA. [7]Institut für Medizinische Mikrobiologie und Hygiene, Institute of Virology, University Medical Center Freiburg, Hermann-Herder-Strasse 11, 79104 Freiburg, Germany. [8]Howard Hughes Medical Institute, Yale School of Medicine, New Haven, CT 06520, USA.
*Present address: Institute of Stem Cell Biology and Regenerative Medicine, School of Medicine, Stanford, CA 94305, USA.
†Corresponding author. Email: akiko.iwasaki@yale.edu

Science

Hobit and Blimp1 instruct a universal transcriptional program of tissue residency in lymphocytes

Laura K. Mackay, Martina Minnich, Natasja A. M. Kragten, Yang Liao, Benjamin Nota, Cyril Seillet, Ali Zaid, Kevin Man, Simon Preston, David Freestone, Asolina Braun, Erica Wynne-Jones, Felix M. Behr, Regina Stark, Daniel G. Pellicci, Dale I. Godfrey, Gabrielle T. Belz, Marc Pellegrini, Thomas Gebhardt, Meinrad Busslinger, Wei Shi, Francis R. Carbone, René A. W. van Lier, Axel Kallies and Klaas P. J. M. van Gisbergen

Science **352** (6284), 459-463.
DOI: 10.1126/science.aad2035

Transcription factors define tissue T cells

The immune system fights microbial invaders by maintaining multiple lines of defense. For instance, specialized memory T cells [resident memory T cells (T_{rms})] colonize portals of pathogen entry, such as the skin, lung, and gut, to quickly halt reinfections. Mackay *et al.* now report that in mice, T_{rms} as well as other tissue-dwelling lymphocyte populations such as natural killer cells share a common transcriptional program driven by the related transcription factors Hobit and Blimp1. Tissue residency and retention of lymphocytes require expression of Hobit and Blimp1, which, among other functions, suppress genes that promote tissue exit.

Science, this issue p. 459

Science (print ISSN 0036-8075; online ISSN 1095-9203) is published by the American Association for the Advancement of Science, 1200 New York Avenue NW, Washington, DC 20005. The title *Science* is a registered trademark of AAAS.